

# Towards an Evolvable Cancer Treatment Simulator

Richard J. Preen<sup>a,\*</sup>, Larry Bull<sup>a</sup>, Andrew Adamatzky<sup>b</sup>

<sup>a</sup>*Department of Computer Science and Creative Technologies*

<sup>b</sup>*Unconventional Computing Laboratory*

*University of the West of England, Bristol, BS16 1QY, UK*

---

## Abstract

The use of high-fidelity computational simulations promises to enable high-throughput hypothesis testing and optimisation of cancer therapies. However, increasing realism comes at the cost of increasing computational requirements. This article explores the use of surrogate-assisted evolutionary algorithms to optimise the targeted delivery of a therapeutic compound to cancerous tumour cells with the multicellular simulator, PhysiCell. The use of both Gaussian process models and multi-layer perceptron neural network surrogate models are investigated. We find that evolutionary algorithms are able to effectively explore the parameter space of biophysical properties within the agent-based simulations, minimising the resulting number of cancerous cells after a period of simulated treatment. Both model-assisted algorithms are found to outperform a standard evolutionary algorithm, demonstrating their ability to perform a more effective search within the very small evaluation budget.

*Keywords:* Agent-based model, evolutionary algorithm, cancer, PhysiCell, high-throughput computing, surrogate modelling

---

## 1. Introduction

PhysiCell ([Ghaffarizadeh et al., 2018](#)) is an open source<sup>1</sup> multicellular simulator based on the biotransport solver, BioFVM ([Ghaffarizadeh et al., 2016](#)). BioFVM simulates substrate secretion, diffusion, uptake, and decay; while PhysiCell models the emergent

---

\*Corresponding author

Email address: [richard2.preen@uwe.ac.uk](mailto:richard2.preen@uwe.ac.uk) (Richard J. Preen)

<sup>1</sup>PhysiCell source code (BSD license): <https://github.com/MathCancer/PhysiCell>

tissue-scale behaviour by simulating cell cycling, death, volume, mechanics, and motility. PhysiCell enables the simulation of new environmental substrates, cell types, and systems of cells, providing a general-purpose toolkit for exploring multicellular systems. Ghaffarizadeh et al. (2018) presented 2-D PhysiCell simulations of targeted cancer drug delivery and 3-D simulations of cancer immunotherapy. Ozik et al. (2018) recently performed a human-selected parameter sweep of 3 values of 3 parameters (27 combinations) on the 3-D cancer immunotherapy simulator with each set sampled 10 times and each simulation requiring  $\approx 2$  days to complete. The results provided insights into therapeutic failure, thus demonstrating the potential of high-throughput computing to investigate high dimensional cancer simulator parameter spaces.

Surrogate model-based optimisation has long been used for global optimisation in applications requiring expensive parameter evaluations, whether via simulated or physical testing (Sacks et al., 1989; Jones et al., 1998; Settles, 2010). Forrester and Keane (2009) present an overview of the process: first the variables to optimise are chosen; some initial parameters are then evaluated; a surrogate (regression) model is selected and used to build a model of the evaluated parameters; followed by a search of the model to identify new parameter values to evaluate; and the newly evaluated parameters added to the existing data. The process loops via continued iterations of model building, searching, and evaluation of selected parameters.

However, given very large high-dimensional search spaces and relatively minuscule evaluation budgets resulting from extremely expensive computational cancer simulations, it may not be possible to perform global optimisation. The use of surrogate modelling has also long been used within evolutionary algorithms (EAs) to reduce the number of costly fitness evaluations (Dunham et al., 1963). As above, a surrogate model,  $y = f(\vec{x})$ , can be formed using a sample  $\mathcal{D}$  of evaluated candidates  $N$ , where  $\vec{x}$  is the genome and  $y$  is the fitness. The model is then used to compute the fitness of unseen data points  $\vec{x} \notin \mathcal{D}$ , thereby providing a cheap approximation of the real fitness function for the EA to use. Both global modelling and local modelling (e.g., using samples within a certain Euclidean distance) are popular approaches (Le et al., 2013). Evaluations with the real fitness function continue to be performed periodically to prevent premature convergence on local optima, known as model management (Jin, 2005; Lim et al., 2010). Jin (2011)

categorised approaches as generational, individual, or population-based, depending upon whether the model is used to evaluate whole generations, samples of individuals within a generation, or sub-populations. The pre-selection approach (Giannakoglou et al., 2001; Ulmer et al., 2003) uses the model to evaluate  $M$  number of offspring and the best of these are chosen for evaluation on the real fitness function. This method has previously been shown effective for the evolution of (noisy) physical systems in which each design is physically instantiated and evaluated for fitness (Preen and Bull, 2015, 2016, 2017). The optimal model management primarily depends upon the testing regime, e.g., whether evaluations can be parallelised.

Many regression models have been used as a surrogate for the real fitness function, including multi-layer perceptron (MLP) based artificial neural networks (e.g., Bull, 1997), Gaussian processes (GP; e.g., Büch et al., 2005; Liu et al., 2014), radial basis functions (RBF; e.g., Regis, 2014), support vector regression (e.g., Yun et al., 2009), sequential parameter optimisation (Bartz-Beielstein, 2006), Markov networks (e.g., Brownlee et al., 2013), and coevolved fitness predictors and training samples (Schmidt and Lipson, 2008). Ensembles, as well as GP global models combined with RBF local models have also been explored (Zhou et al., 2007). Preen and Bull (2016) showed that with very small and noisy samples there is little difference between the modelling approaches, with MLPs appearing to be a robust approach capable of capturing the underlying structure of the search space.

Four main categories of uncertainty (or noise) are frequently encountered in real-world optimisation problems (Jin and Branke, 2005):

1. Uncertainty in the objective function evaluation. This is common in stochastic simulations and physical systems where evaluations with the same parameters produce different results, e.g., by sensory measurement errors. Efficiently reducing the objective function error requires optimally selecting how many samples to perform for a given parameter set. Issues such as how best to aggregate the results, e.g., by mean or median may also affect convergence.
2. The objective function is approximated by a surrogate model. Efficiently reducing the model error requires optimally selecting which samples to evaluate with the real objective function to provide new training data and avoidance of over-fitting

through validation (Bischl et al., 2012). Approximated objective values are also encountered where the function evaluations take place over time and partial fitness scores can be observed by early termination (Park et al., 2013).

3. Dynamic optimisation wherein the objectives change over time (e.g., Yang and Yao, 2013).
4. Robust optimisation (e.g., Ong et al., 2006) which seeks solutions that are less sensitive to small parameter perturbations, e.g., due to manufacturing tolerances. This typically involves a trade-off between solution quality and robustness.

Rakshit et al. (2017) present a recent overview on techniques for dealing with noisy evolutionary optimisation. Uncertainty in the objective function can be addressed via the explicit averaging of resampled parameters or implicit averaging using a large population size. The evolutionary selection mechanism may also be modified to account for noisy evaluations; for example, by only accepting offspring with observed fitness greater than the parent’s plus some threshold (Markon et al., 2001). The number of samples to perform for a given parameter set can either remain fixed (static) for all candidate solutions or be dynamically allocated to each, e.g., based on the sample variance (Siegmund et al., 2013).

## 2. Physics-based Multicellular Simulations

### 2.1. Methodology

Many proposed cancer therapies attempt to target malignant cells by finding specific surfaces or molecules in order that drugs can be conjugated to custom antibodies or encapsulated in custom nanoparticles. The PhysiCell 2-D anti-cancer biorobots simulation (Ghaffarizadeh et al., 2018) enables the high-throughput testing of a simple targeted drug delivery therapy in which three types of cells are modelled:

- Oxygen consuming cancer cells that generate a chemoattractant  $c_1$  forming an oxygen gradient which can be used to guide worker cells.
- Worker cells that may adhere to cargo cells. Each cell has a persistence time, migration speed, migration direction, and migration bias. Worker cells perform a

biased random migration towards cancer cells when adhered to cargo, and a biased random migration towards cargo cells when unadhered. Migration biases range  $[0,1]$  with 0 representing Brownian motion and 1 deterministic motion. The motility of unadhered worker cells is disabled if  $c_1$  falls below a threshold.

- Cargo cells that secrete a diffusible chemoattractant  $c_2$  used to guide worker cells. Adhered cargo cells detach from worker cells and secrete a therapeutic compound that induces apoptosis in nearby tumour cells when oxygenation falls below the cargo release  $o_2$  threshold.

Each simulation is initialised with a 200 micron radius tumour. After 7 simulated days of tumour growth, 500 cells are “injected” near the tumour: 10% worker cells and 90% cargo cells. The simulation subsequently continues for 3 additional days of cancer therapy. A single simulation requires  $\approx 5$  minutes of wall-clock time on an Intel<sup>®</sup> Xeon<sup>®</sup> CPU E5-2650 v4 @ 2.20GHz with 64GB RAM using half of the 48 cores. Here we use an EA to optimise  $N = 6$  parameters specifying worker agent characteristics and cargo properties. All other parameters remain at their original values as shown in Table 1.

In particular, we explore the attached worker migration bias  $[0,1]$ ; the unattached worker migration bias  $[0,1]$ ; worker relative adhesion  $[0,10]$ ; worker relative repulsion  $[0,10]$ ; worker motility persistence time (minutes)  $[0,10]$ ; and the cargo release  $o_2$  threshold (mmHg)  $[0,20]$ . A steady-state genetic algorithm with population size  $P = 20$  is used; tournament size  $T = 3$  for both selection and replacement; uniform crossover is performed with  $\mathcal{X} = 80\%$  probability; and a per allele mutation rate  $\mu = 1/N$  with a uniform random step size  $s = [-5, 5]\%$ . A static sampling approach is used wherein  $k$  simulation runs are performed for each candidate solution before assigning the fitness as the mean number of remaining cells after 7 simulated days of tumour growth plus 3 days of targeted drug delivery.

Initially all individuals in the initial population are evaluated and a regression model fit. Subsequently, evolution proceeds by iteratively selecting 2 parents (as usual) and then creating and evaluating  $M = 1000$  offspring with the model. The most promising of these is then selected for evaluation by the multicellular simulator and replaces an individual in the population selected via a negative tournament. Finally, the evaluated archive set is updated and the model retrained. We explore the use of both GP (Rasmussen and

Table 1: Default multicellular simulation parameters.

Maximum attachment distance	18 microns
Minimum attachment distance	14 microns
Worker apoptosis rate	0 minutes <sup>-1</sup>
Worker migration speed	2 microns/minute
Worker o <sub>2</sub> relative uptake	0.1 minutes <sup>-1</sup>
Cargo o <sub>2</sub> relative uptake	0.1 minutes <sup>-1</sup>
Cargo apoptosis rate	4.065e-5 minutes <sup>-1</sup>
Cargo relative adhesion	0
Cargo relative repulsion	5
Damage rate	0.03333 minutes <sup>-1</sup>
Repair rate	0.004167 minutes <sup>-1</sup>
Drug death rate	0.004167 minutes <sup>-1</sup>
Maximum relative cell adhesion distance	1.25
Elastic coefficient	0.05 minutes <sup>-1</sup>
Maximum elastic displacement	50 microns
Motility shutdown detection threshold	0.001
Attachment receptor threshold	0.1

(Williams, 2006) surrogate models using the expected improvement (EI; Jones et al., 1998) as the rating (acquisition) function to select the next offspring, and MLP models using the best predicted fitness for rating. The EI criterion combines the model standard deviation with the mean prediction to explore regions of both high promise and high uncertainty (Ulmer et al., 2003). Here, the GP model uses a radial basis kernel function and the MLP uses  $H = 10$  rectified linear units in the hidden layer and is trained using the limited-memory Broyden-Fletcher-Goldfarb-Shanno (L-BFGS) quasi-Newton optimisation algorithm (Fletcher, 1987). All experiments are initialised with the same randomly generated population. Algorithm 1 outlines the surrogate-assisted EA with static sampling and Algorithm 2 shows the expected improvement rating function used for the GP model. For the MLP model, *Rating()* returns the model predicted fitness.

## 2.2. Results

Since each simulation run is costly, we initially explored the case with  $k = 1$ . However, after 400 evaluations/simulations, the performance of the fittest individual discovered by the EA was not significantly different than the fittest individual in the initial population,  $p > 0.05$  using a Wilcoxon rank-sums test, showing that the EA is severely misled by the significant variance in simulation runs with the same parameter set.

Figure 1 shows the mean number of cells resulting from the fittest individual discovered for each algorithm with  $k = 10$ . After evaluating 200 candidates (2000 simulations), the best GP-assisted solution (mean = 852.10, SD = 40.43, samples = 10, min = 773, median = 870, kurtosis = -0.89) and the best MLP-assisted solution (mean = 852.20, SD = 39.84, samples = 10, min = 791, median = 853, kurtosis = -0.74) are significantly less than the best EA solution without surrogate assistance (mean = 889.30, SD = 32.75, samples = 10, min = 831, median = 898, kurtosis = -0.83),  $p \leq 0.05$  using a Wilcoxon rank-sums test. There is no significant difference between the surrogate models. All algorithms found solutions with a significantly lower mean number of cells than the best individual in the initial population (mean = 953.50, SD = 41.59, samples = 10, min = 887, median = 947, kurtosis = -1.10),  $p \leq 0.05$ .

Figure 2 shows scatter plots of all evaluated individuals for each evolved parameter. As can be seen, both surrogate-assisted EAs identified best solutions with a mean of 852 cells and these solutions have similar values for 4 of the parameters:  $\approx 0.5$  unattached worker migration bias;  $\approx 6$  worker relative adhesion;  $\approx 10$  worker motility persistence time; and  $\approx 11$  cargo release  $\text{o}_2$  threshold. However, the MLP-assisted model achieved this with an attached worker migration bias of 0.89, whereas the GP-assisted solution was 0.29. Additionally, the worker relative repulsion was 5.9, compared with 1.13 for the GP-assisted model.

There appears to be a clear funnel with a minimum at  $\approx 11$  for the cargo release  $\text{o}_2$  threshold, suggesting that this is the global optima for the parameter. Ghaffarizadeh et al. (2018) used an initial cargo release  $\text{o}_2$  threshold of 10, finding that “once enough cancer cells were killed, hypoxia was reduced so that worker cells clustered near the oxygen minimum, but no longer released their cargo”. Increasing the threshold to 15 “reduced but did not eliminate this behaviour”. The results of these simulations suggest

that using a threshold of 11 results in the best performance. As [Ghaffarizadeh et al. \(2018\)](#) note, “the cargo release rules need to be carefully engineered. Such a system could potentially activate and deactivate to keep a tumour cell population in control, and to reduce hypoxia [which is known to drive cancer cell adaptation to more aggressive phenotypes ([Wilson and Hay, 2011](#); [Eales et al., 2016](#))]”.

An example run of the fittest evolved individual with the GP-surrogate model is shown in [Figure 3](#), showing that the worker cells appear to disperse evenly and effectively deliver the cargo to the tumour.

### 3. Conclusions

This article has shown that EAs are able to effectively explore the parameter space of biophysical properties within the agent-based multicellular simulator, PhysiCell. EAs successfully minimised the number of cancerous cells after a period of simulated treatment. Both surrogate-assisted algorithms were found to outperform the standard EA, demonstrating an ability to reduce the number of expensive simulations required with a very small evaluation budget.

### Acknowledgement

This work was supported by the European Research Council under the European Union’s Horizon 2020 research and innovation programme under grant agreement No. 800983.

### References

- Bartz-Beielstein, T., 2006. Experimental Research in Evolutionary Computation. Natural Computing Series, Springer-Verlag, Berlin, Germany. doi:[10.1007/3-540-32027-X](#).
- Biscl, B., Mersmann, O., Trautmann, H., Weihs, C., 2012. Resampling methods for meta-model validation with recommendations for evolutionary computation. *Evol. Comput.* 20, 249–275. doi:[10.1162/EVC0\\_a\\_00069](#).
- Brownlee, A.E.I., McCall, J.A.W., Zhang, Q., 2013. Fitness modeling with Markov networks. *IEEE Trans. Evol. Comput.* 17, 862–879. doi:[10.1109/TEVC.2013.2281538](#).



- Büch, D., Schraudolph, N.N., Koumoutsakos, P., 2005. Accelerating evolutionary algorithms with Gaussian process fitness function models. *IEEE Trans. Syst., Man, Cybern. C* 35, 183–194. doi:[10.1109/TSMCC.2004.841917](https://doi.org/10.1109/TSMCC.2004.841917).
- Bull, L., 1997. Model-based evolutionary computing: A neural network and genetic algorithm architecture, in: *Proc. IEEE Int. Conf. Evol. Comput.*, pp. 611–616. doi:[10.1109/ICEC.1997.592384](https://doi.org/10.1109/ICEC.1997.592384).
- Dunham, B., Fridshal, R., North, J.H., 1963. Design by natural selection. *Synthese* 15, 254–259. doi:[10.1007/BF00484855](https://doi.org/10.1007/BF00484855).
- Eales, K.L., Hollinshead, K.E.R., Tennant, D.A., 2016. Hypoxia and metabolic adaptation of cancer cells. *Oncogenesis* 5, e190. doi:[10.1038/oncsis.2015.50](https://doi.org/10.1038/oncsis.2015.50).
- Fletcher, R., 1987. *Practical methods of optimization*. 2 ed., John Wiley & Sons, New York, NY, USA.
- Forrester, A.I.J., Keane, A.J., 2009. Recent advances in surrogate-based optimization. *Prog. Aerosp. Sci.* 45, 50–79. doi:[10.1016/j.paerosci.2008.11.001](https://doi.org/10.1016/j.paerosci.2008.11.001).
- Ghaffarizadeh, A., Friedman, S.H., Macklin, P., 2016. BioFVM: An efficient, parallelized diffusive transport solver for 3-D biological simulations. *Bioinformatics* 32, 1256–1258. doi:[10.1093/bioinformatics/btv730](https://doi.org/10.1093/bioinformatics/btv730).
- Ghaffarizadeh, A., Heiland, R., Friedman, S.H., Mumenthaler, S.M., Macklin, P., 2018. PhysiCell: An open source physics-based cell simulator for 3-D multicellular systems. *PLoS Comput. Biol.* 14, 1–31. doi:[10.1371/journal.pcbi.1005991](https://doi.org/10.1371/journal.pcbi.1005991).
- Giannakoglou, K.C., Giotis, A.P., Karakasis, M.K., 2001. Low-cost genetic optimization based on inexact pre-evaluations and the sensitivity analysis of design parameters. *Inverse Probl. Eng.* 9, 389–412. doi:[10.1080/174159701088027771](https://doi.org/10.1080/174159701088027771).
- Jin, Y., 2005. A comprehensive survey of fitness approximation in evolutionary computation. *Soft Comput.* 9, 3–12. doi:[10.1007/s00500-003-0328-5](https://doi.org/10.1007/s00500-003-0328-5).
- Jin, Y., 2011. Surrogate-assisted evolutionary computation: Recent advances and future challenges. *Swarm Evol. Comput.* 1, 61–70. doi:[10.1016/j.swevo.2011.05.001](https://doi.org/10.1016/j.swevo.2011.05.001).
- Jin, Y., Branke, J., 2005. Evolutionary optimization in uncertain environments—A survey. *IEEE Trans. Evol. Comput.* 9, 303–317. doi:[10.1109/TEVC.2005.846356](https://doi.org/10.1109/TEVC.2005.846356).
- Jones, D.R., Schonlau, M., Welch, W.J., 1998. Efficient global optimization of expensive black-box functions. *J. Global Optim.* 13, 455–492. doi:[10.1023/A:1008306431147](https://doi.org/10.1023/A:1008306431147).
- Le, M.N., Ong, Y.S., Menzel, S., Jin, Y., Sendhoff, B., 2013. Evolution by adapting surrogates. *Evol. Comput.* 21, 313–340. doi:[10.1162/EVCO\\_a\\_00079](https://doi.org/10.1162/EVCO_a_00079).
- Lim, D., Jin, Y., Ong, Y.S., Sendhoff, B., 2010. Generalizing surrogate-assisted evolutionary computation. *IEEE Trans. Evol. Comput.* 14, 329–355. doi:[10.1109/TEVC.2009.2027359](https://doi.org/10.1109/TEVC.2009.2027359).
- Liu, B., Zhang, Q., Gielen, G.G.E., 2014. A Gaussian process surrogate model assisted evolutionary algorithm for medium scale expensive optimization problems. *IEEE Trans. Evol. Comput.* 18, 180–192. doi:[10.1109/TEVC.2013.2248012](https://doi.org/10.1109/TEVC.2013.2248012).
- Markon, S., Arnold, D.V., Bäck, T., Beielstein, T., Beyer, H.G., 2001. Thresholding—A selection operator for noisy ES, in: *Proc. IEEE Congr. Evol. Comput.*, IEEE Press, Piscataway, NJ, USA. pp. 465–472. doi:[10.1109/CEC.2001.934428](https://doi.org/10.1109/CEC.2001.934428).

- Ong, Y.S., Nair, P.B., Lum, K.Y., 2006. Max-min surrogate-assisted evolutionary algorithm for robust design. *IEEE Trans. Evol. Comput.* 10, 392–404. doi:[10.1109/TEVC.2005.859464](https://doi.org/10.1109/TEVC.2005.859464).
- Ozik, J., Collier, N.T., Wozniak, J.M., Macal, C.M., Cockrell, C., Friedman, S.H., Ghaffarizadeh, A., Heiland, R., An, G., Macklin, P., 2018. High-throughput cancer hypothesis testing with an integrated PhysiCell-EMEWS workflow. *BMC Bioinformatics* In press.
- Park, N., Kim, K., McKay, R.I., 2013. Cutting evaluation costs: An investigation into early termination in genetic programming, in: *Proc. IEEE Congr. Evol. Comput.*, IEEE Press, Piscataway, NJ, USA. pp. 3291–3298. doi:[10.1109/CEC.2013.6557973](https://doi.org/10.1109/CEC.2013.6557973).
- Preen, R.J., Bull, L., 2015. Toward the coevolution of novel vertical-axis wind turbines. *IEEE Trans. Evol. Comput.* 19, 284–294. doi:[10.1109/TEVC.2014.2316199](https://doi.org/10.1109/TEVC.2014.2316199).
- Preen, R.J., Bull, L., 2016. Design mining interacting wind turbines. *Evol. Comput.* 24, 89–111. doi:[10.1162/EVC0\\_a\\_00144](https://doi.org/10.1162/EVC0_a_00144).
- Preen, R.J., Bull, L., 2017. On design mining: Coevolution and surrogate models. *Artif. Life* 23, 186–205. doi:[10.1162/ARTL\\_a\\_00225](https://doi.org/10.1162/ARTL_a_00225).
- Rakshit, P., Konar, A., Das, S., 2017. Noisy evolutionary optimization algorithms – A comprehensive survey. *Swarm Evol. Comput.* 33, 18–45. doi:[10.1016/j.swevo.2016.09.002](https://doi.org/10.1016/j.swevo.2016.09.002).
- Rasmussen, C.E., Williams, C.K.I., 2006. *Gaussian Processes for Machine Learning*. MIT Press, Cambridge, MA, USA.
- Regis, R.G., 2014. Evolutionary programming for high-dimensional constrained expensive black-box optimization using radial basis functions. *IEEE Trans. Evol. Comput.* 18, 326–347. doi:[10.1109/TEVC.2013.2262111](https://doi.org/10.1109/TEVC.2013.2262111).
- Sacks, J., Welch, W.J., Mitchell, T.J., Wynn, H.P., 1989. Design and analysis of computer experiments. *Stat. Sci.* 4, 409–435.
- Schmidt, M.D., Lipson, H., 2008. Coevolution of fitness predictors. *IEEE Trans. Evol. Comput.* 12, 736–749. doi:[10.1109/TEVC.2008.919006](https://doi.org/10.1109/TEVC.2008.919006).
- Settles, B., 2010. *Active Learning Literature Survey*. Technical Report 1648. Department of Computer Science, University of Wisconsin-Madison. Madison, WI, USA.
- Siegmund, F., Ng, A.C.H., Deb, K., 2013. A comparative study of dynamic resampling strategies for guided evolutionary multi-objective optimization, in: *Proc. IEEE Congr. Evol. Comput.*, IEEE Press, Piscataway, NJ, USA. pp. 1826–1835. doi:[10.1109/CEC.2013.6557782](https://doi.org/10.1109/CEC.2013.6557782).
- Ulmer, H., Streichert, F., Zell, A., 2003. Evolution strategies assisted by Gaussian processes with improved preselection criterion, in: *Proc. IEEE Congr. Evol. Comput.*, IEEE Press, Piscataway, NJ, USA. pp. 692–699. doi:[10.1109/CEC.2003.1299643](https://doi.org/10.1109/CEC.2003.1299643).
- Wilson, W.R., Hay, M.P., 2011. Targeting hypoxia in cancer therapy. *Nat. Rev. Canc.* 11, 393–410. doi:[10.1038/nrc3064](https://doi.org/10.1038/nrc3064).
- Yang, S., Yao, X. (Eds.), 2013. *Evolutionary Computation for Dynamic Optimization Problems*. Studies in Computational Intelligence, Springer-Verlag, Berlin, Germany. doi:[10.1007/978-3-642-38416-5](https://doi.org/10.1007/978-3-642-38416-5).
- Yun, Y., Yoon, M., Nakayama, H., 2009. Multi-objective optimization based on meta-modeling by using support vector regression. *Opt. Eng.* 10, 167–181. doi:[10.1007/s11081-008-9063-1](https://doi.org/10.1007/s11081-008-9063-1).

Zhou, Z., Ong, Y.S., Nair, P.B., Keane, A.J., Lum, K.Y., 2007. Combining global and local surrogate models to accelerate evolutionary optimization. *IEEE Trans. Evol. Comput.* 37, 66–76. doi:[10.1109/TSMCC.2005.855506](https://doi.org/10.1109/TSMCC.2005.855506).

---

**Algorithm 1:** Surrogate-assisted EA with pre-selection and static sampling

---

```
1  $N = 6, P = 20, k = 10, M = 1000, \mathcal{X} = 0.8, \mu = 1/N, s = 0.1, T = 3$ 
2 Initialise population  $Pop = \{\vec{x}_1, \dots, \vec{x}_P\}$  //  $\vec{x}$  normalised  $[-1,1]$ 
3 Evaluate  $Pop$  with the real objective function  $k$  times and add to archive  $\mathcal{A}$ 
4 while evaluation budget not exhausted do
    /* build surrogate model */
5    Fit regression model  $\mathcal{R}$  using  $\mathcal{A}$ 
    /* pre-select offspring */
6    Parent  $p_1 \leftarrow \text{TournamentSelection}(Pop, T)$ 
7    Parent  $p_2 \leftarrow \text{TournamentSelection}(Pop, T)$ 
8    for  $M$  number of offspring do
9        Offspring  $a \leftarrow p_1$ 
        /* crossover */
10       if  $\text{Random}(0,1) < \mathcal{X}$  then
11           | Perform uniform crossover with  $a$  and  $p_2$ 
12       end
        /* mutation */
13       for each parameter  $x$  in  $a$  do
14           | if  $\text{Random}(0,1) < \mu$  then
15               |  $x \leftarrow x + \text{Random}(-s, s)$ 
16           | end
17       end
        /* evaluate offspring with surrogate model */
18        $a.\text{utility} \leftarrow \text{Rating}(\mathcal{R}, a, \mathcal{A})$ 
19   end
    /* select, evaluate, and add the most promising offspring */
20   Evaluate the best utility offspring with the real objective function  $k$  times
21   Add offspring to  $\mathcal{A}$ 
22    $r \leftarrow \text{NegativeTournamentSelection}(Pop, T)$ 
23   Replace  $r$  with offspring
24 end
```

---

---

**Algorithm 2:** Expected improvement rating function

---

```
1 Input: fitted regression model  $\mathcal{R}$ , candidate  $a$ , evaluated archive  $\mathcal{A}$ 
2 Output: model expected improvement of  $a$ 
3  $ei \leftarrow 0$ 
4  $mean, std \leftarrow \mathcal{R}.predict(a)$ 
5 if  $std \neq 0$  then
6    $imp \leftarrow BestFitness(\mathcal{A}) - mean$  // minimising
7    $z \leftarrow imp/std$ 
8   /*  $cdf()$  is the standard normal cumulative distribution function */
9   /*  $pdf()$  is the standard normal probability density function */
10   $ei \leftarrow imp \times cdf(z) + std \times pdf(z)$ 
11 end
12 return  $ei$ 
```

---

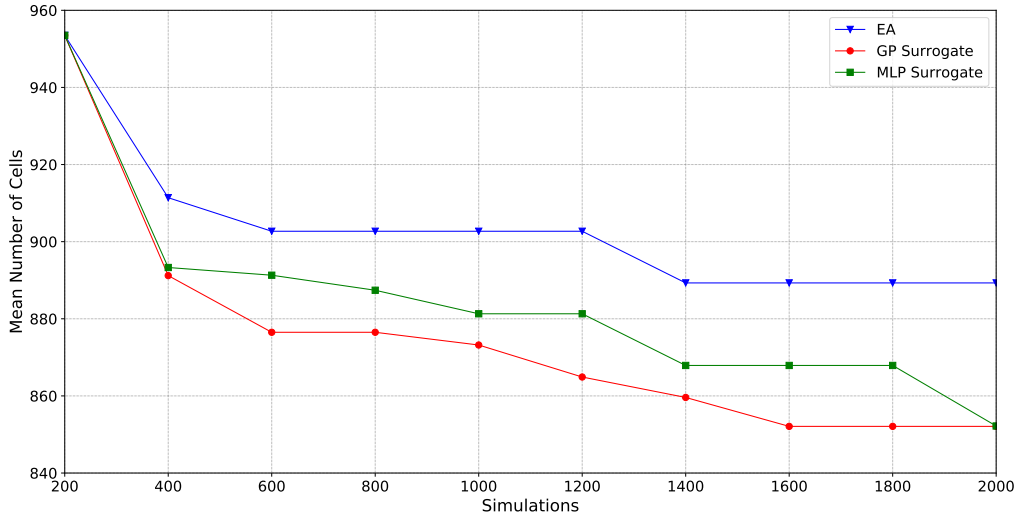


Figure 1: Fittest individuals on the PhysiCell anti-cancer biorobots simulator. EA (triangle), GP-assisted EA (circle), and MLP-assisted EA (square).

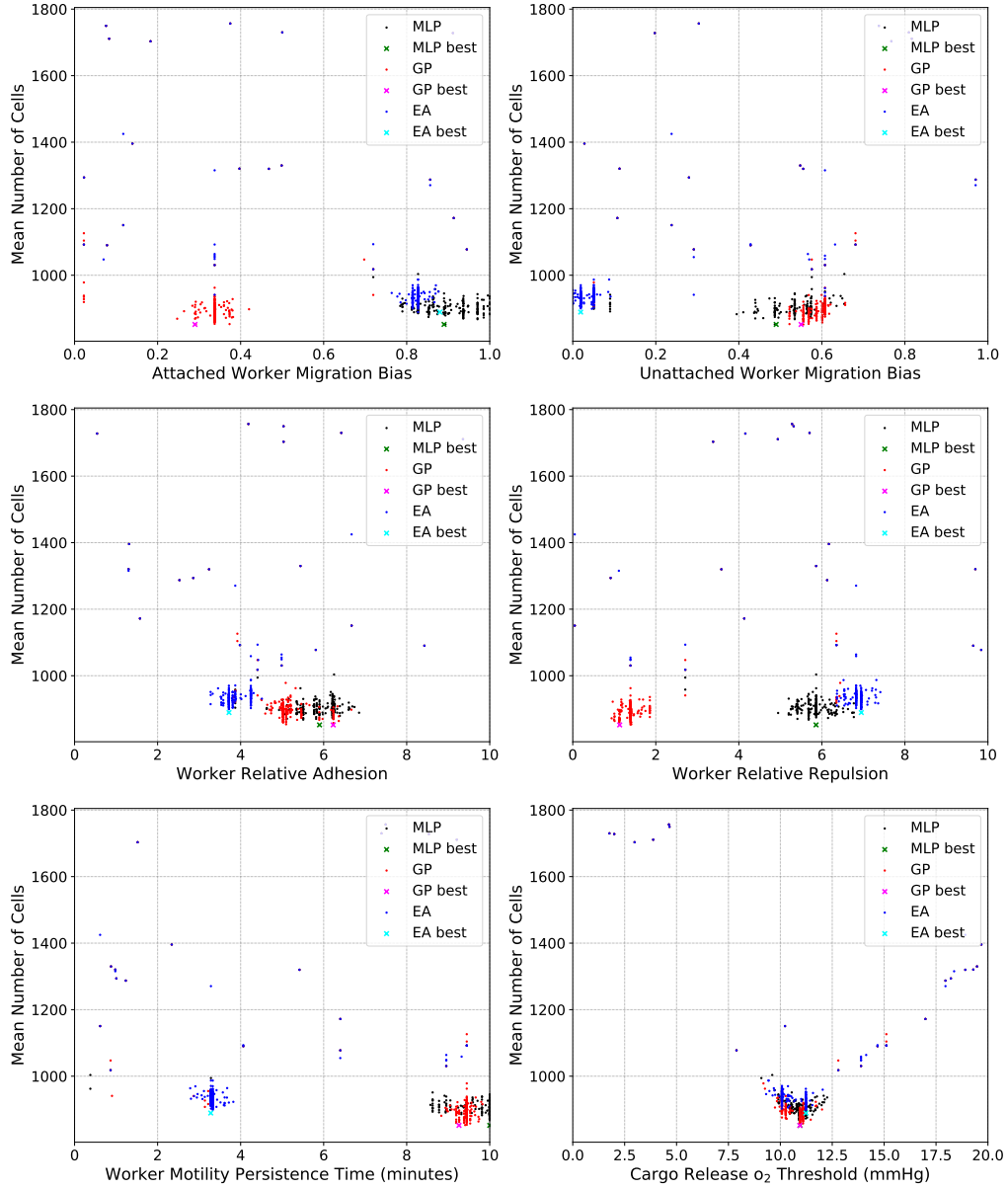


Figure 2: Scatter plot of all evaluated individuals on the PhysiCell anti-cancer biorobots simulator.

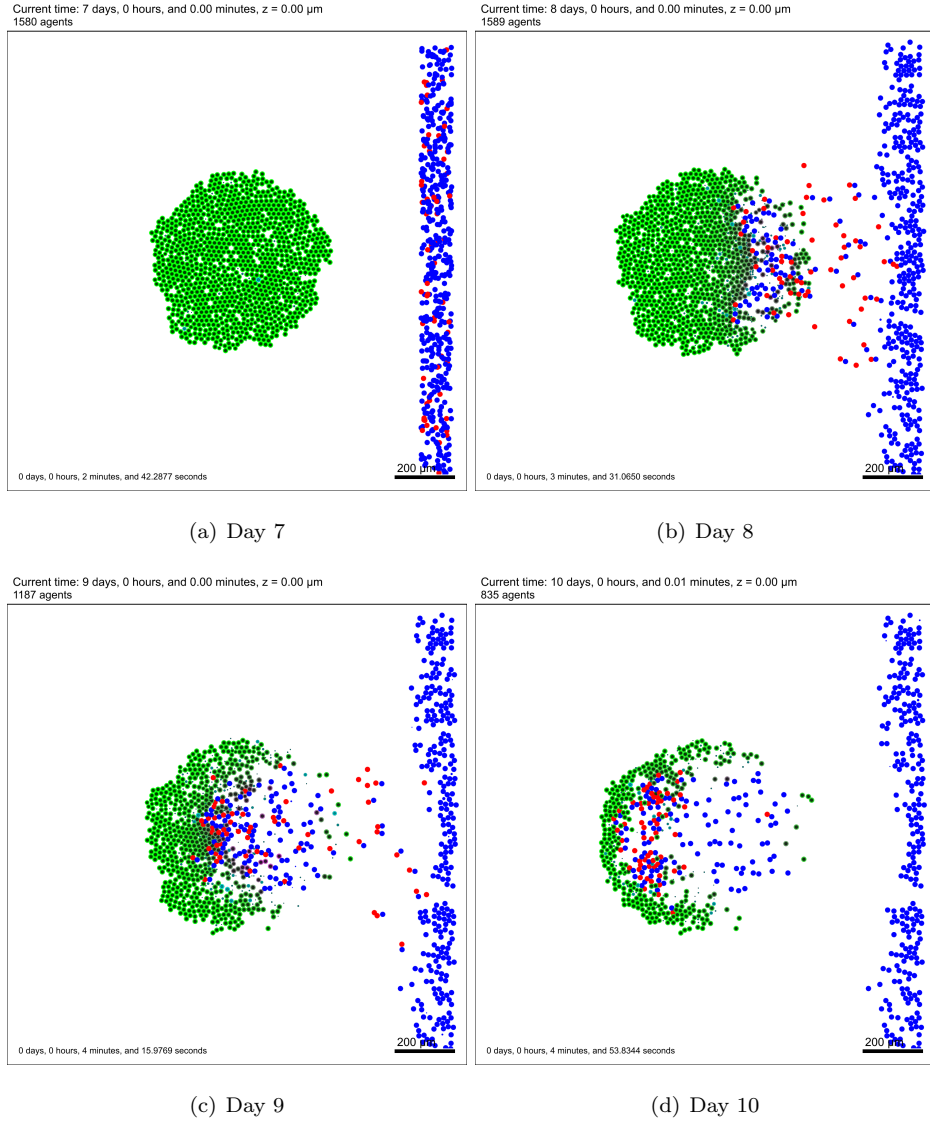


Figure 3: Example run of the fittest evolved individual with the GP-surrogate model on the PhysiCell anti-cancer biorobots simulator after 200 candidate evaluations (2000 simulations.) Shown are the worker cells (red), cargo cells (blue), and tumour cells (green) after 7 days of tumour growth and each subsequent day of treatment. Attached worker migration bias = 0.29; unattached worker migration bias = 0.55; worker relative adhesion = 6.24; worker relative repulsion = 1.13; worker motility persistence time = 9.26; cargo release  $\text{o}_2$  threshold = 10.94. Mean number of cells after 10 simulated days = 852.